Supplemental Information:
Multi-flavor quantum criticality

A. Khansili,[1] A. Bangura,[2] R. D. McDonald,[3] B. J. Ramshaw,[4] A. Rydh,[1] and A. Shekhter[3]

[1]*Department of Physics, Stockholm University, SE-106 91 Stockholm, Sweden*

[2]*National High Magnetic Field Laboratory, Tallahassee FL*

[3]*Los Alamos National Laboratory, Los Alamos NM*

[4]*Laboratory of Atomic and Solid State Physics,*

Cornell University, Ithaca NY 14853 USA

(Dated: December 2, 2023)

Supplementary Figure S1:

Comparison of zero field C/T

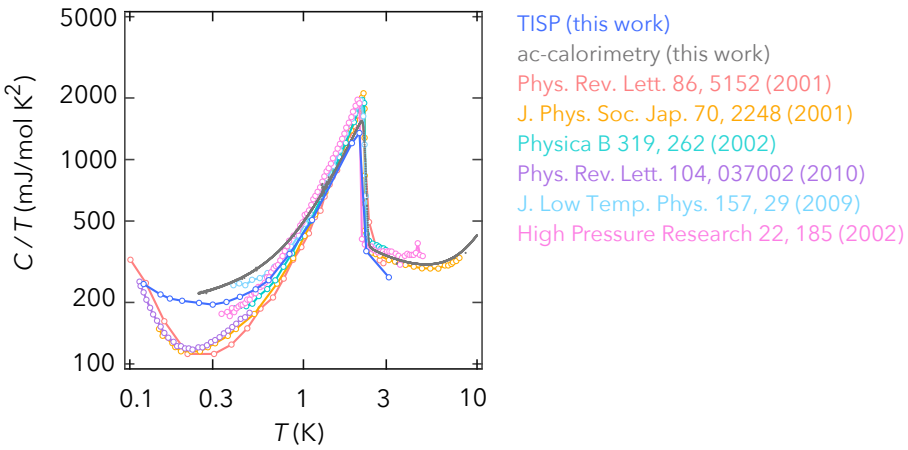

FIG. S1. **Comparison of C/T of $CeCoIn_5$ at zero field.** Measurements in this work (TISP: open blue circles, AC calorimetry: black dots) are compared with measurements from References [1–6]. Over the temperature range of 0.6 K to 2 K, all measurements fall within 10% of each other.

Supplementary Figure S2:

Evaluation of T_α at 12 T

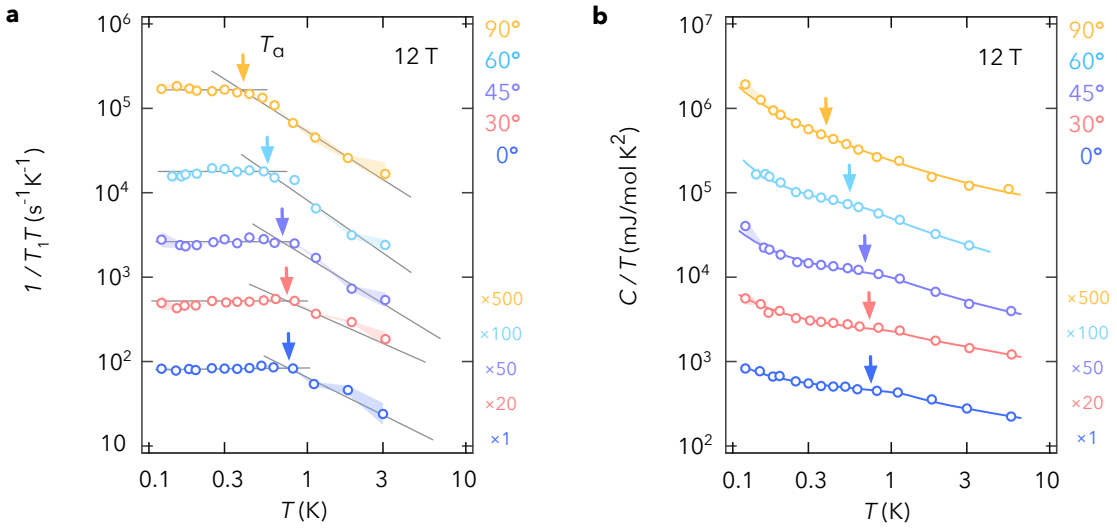

FIG. S2. **Evaluation of T_α at 12 T. a.** $1/T_1T$ in Fig. 1d in the main text, shifted vertically to highlight the crossover region for each temperature sweep. Thin gray lines indicate the limiting behavior below and above crossover T_α. The value of T_α is determined as the crossing point of the two gray lines, as indicated by the arrow. **b.** C/T in Fig. 1c in the main text shifted vertically for clarity. The location of T_α, as determined by analysis of $1/T_1T$ in panel a, are shown as arrows.

Supplementary Figure S3:

Evaluation of T_α and T_c for different magnetic fields and field orientations

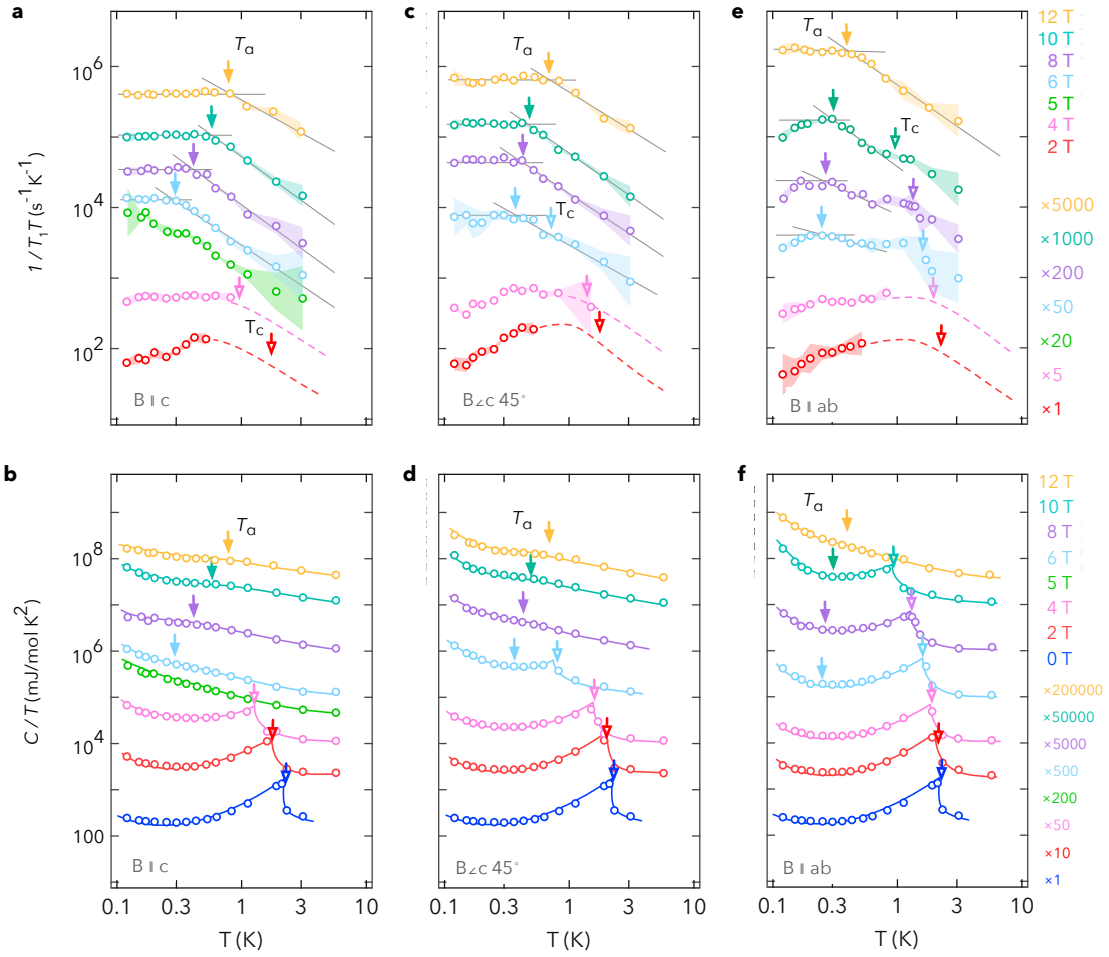

FIG. S3. **Evaluation of T_α and T_c for different orientations and magnitudes of magnetic fields. a,c,e.** Temperature dependence of $1/T_1T$ from Fig. 2 in the main text at different magnetic fields, offset vertically for clarity. Solid gray lines indicate the limiting behavior above and below the crossover temperature T_α, similar to Fig. S2. The crossover temperature T_α is determined as their intercept, indicated by the solid arrow. The color shading indicates the fitting error bars as described in the Methods of the main text. **b,d,f.** Corresponding specific heat of Fig. 2 of the main text. The open arrows indicate the superconducting transition temperature. T_α, as determined from $1/T_1T$, are shown as solid arrows.

Supplementary Figure S4:

Magnetic field dependence of $T_\alpha(B)$ and $T_c(B)$

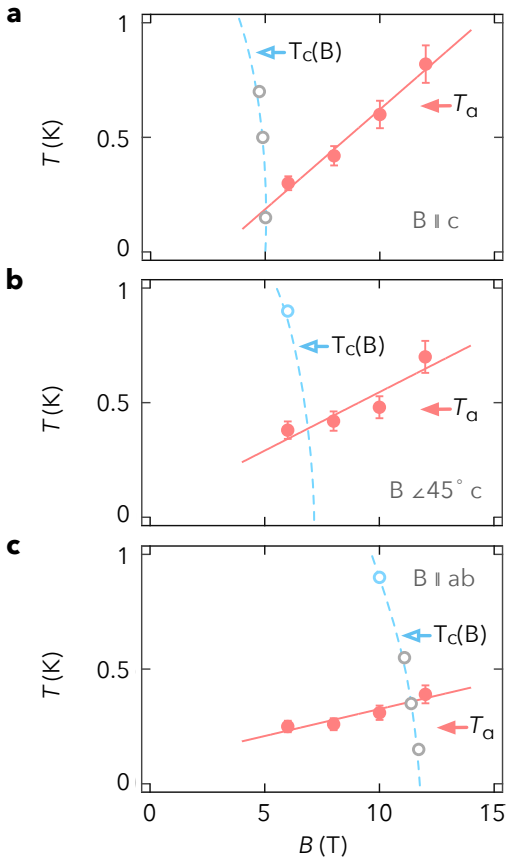

FIG. S4. **Magnetic field dependence of T_α and $T_c(B)$. a,b,c.** Magnetic field dependence of $T_\alpha(B)$ and $T_c(B)$ for magnetic fields along the c-axis, at $B\angle 45°$, and along the ab-plane, respectively. See also Fig. 3 of the main text.

Supplementary Figure S5:

Determination of q-factors

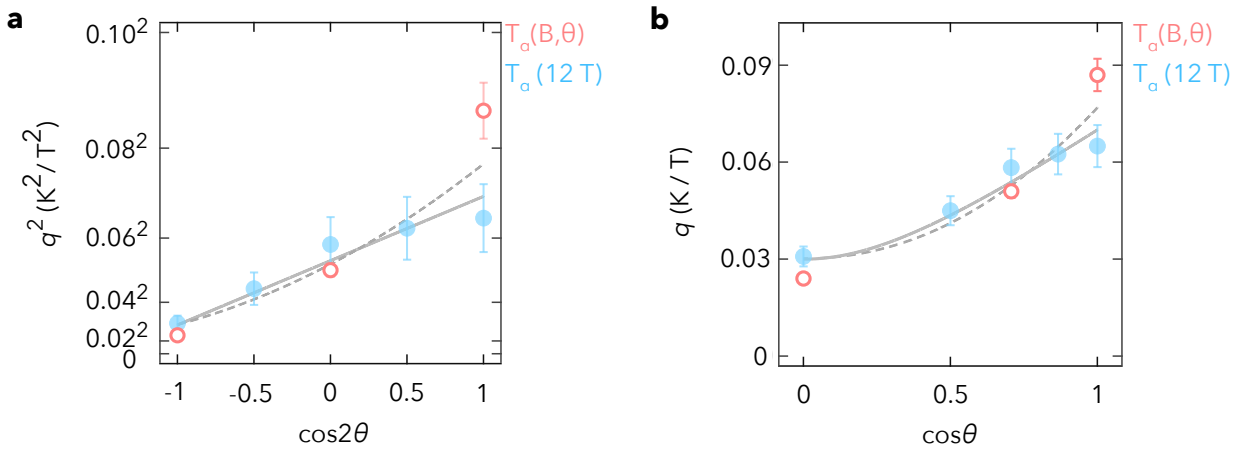

FIG. S5. **Determination of q-factors. a.** Angular dependence of $q^2(\theta)$ vs $\cos 2\theta$ determined as $q^2(\theta) = (T_\alpha/B)^2$ in Fig. S2 and from the slopes in Fig. S4 using $q^2(\theta) \approx (dT_\alpha/dB)^2$. The approximate linear dependence is consistent with lowest-angular-harmonic behavior of the tetragonal lattice structure of $CeCoIn_5$, $q^2(\theta) = q_c^2 \cos^2\theta + q_{ab}^2 \sin^2\theta$, or, equivalently $q^2(\theta) = {}^1\!/_2(q_c^2 + q_{ab}^2) + {}^1\!/_2(q_c^2 - q_{ab}^2)\cos 2\theta$. The linear regression of the data in panel a produces ${}^1\!/_2(q_c^2 + q_{ab}^2) = 2.9(5)$ (mK/T)^2 and ${}^1\!/_2(q_c^2 - q_{ab}^2) = 2.0(2)$ (mK/T)^2. This corresponds to $q_c = 70(5)$ mK/T and $q_{ab} = 30(5)$ mK/T. The solid line represents the linear fit. The dotted curve corresponds to the best-fit with the second and fourth harmonics, $q^2(\theta) = a + b\cos 2\theta + c\cos 4\theta$ with parameters $a = 3.1(5)$ (mK/T)^2, $b = 2.5(2)$ (mK/T)^2, and $c = 0.30(2)$ (mK/T)^2. Such higher order harmonic fit changes the values of the q-factors to $q_c = 75(5)$ mK/T and $q_{ab} = 25(5)$ mK/T. **b.** $q(\theta)$ plotted vs $\cos\theta$. Solid curve represents the lowest harmonic approximation, $q(\theta) = (q_c^2\cos^2\theta + q_{ab}^2\sin^2\theta)^{1/2}$ with q_c and q_{ab} determined by linear regression in panel a. The dotted curve represents the the best-fit for the fourth harmonic approximation.

Supplementary Figure S6:

Normalized C/T for different magnetic fields and field orientations

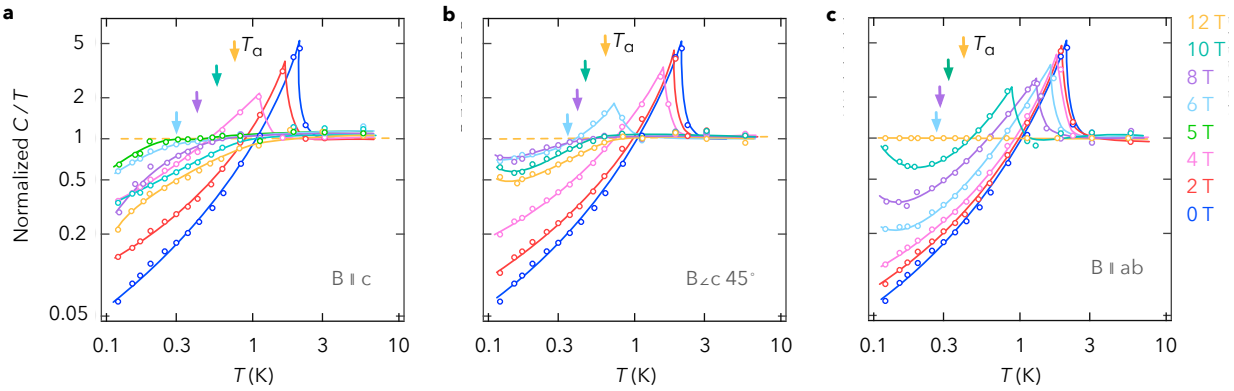

FIG. S6. **Normalized C/T for different magnetic fields and field orientations. a,b,c.** Electronic C/T divided by C/T at 12 T along the ab-plane in the normal state. The arrows represent the crossover temperature $T_\alpha(B)$ determined in Fig. S3.

Supplementary Note 1:

Two nuclear components in $CeCoIn_5$

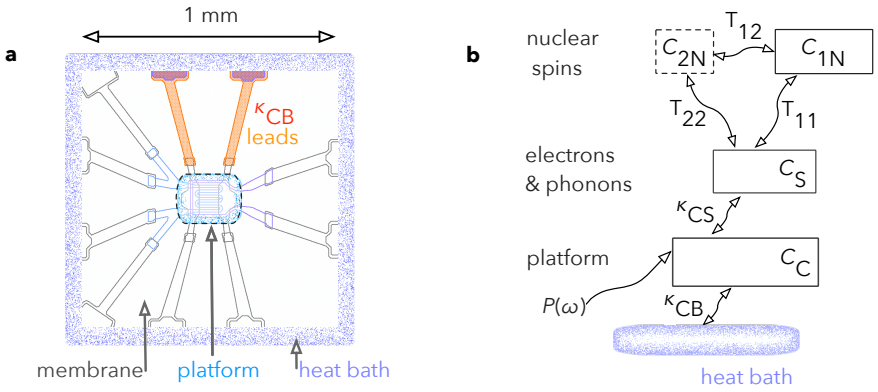

FIG. S7. **Heat flow diagram of the calorimeter-sample asembly with two nuclear components. a.** A sketch of the calorimeter, indicating different components. **b.** Heat flow diagram of the calorimeter-sample assembly which determines the thermal impedance in Eq. (S1). $CeCoIn_5$ has two nuclear spin subsystems, that of $^{115/113}$In (C_{1N}) and that of ^{59}Co (C_{2N}).

The model described in the Methods of the main text accounts for a single nuclear isotope species coupled to the electrons via the nuclear spin lattice relaxation rate $1/T_1$. In $CeCoIn_5$, about 13% of the nuclear heat capacity comes from ^{59}Co while the rest comes from $^{115/113}$In. The resulting two-nuclear-component heat circuit is described by a larger (9-parameter) model,

$$\frac{1}{\zeta(\omega)_2^{\text{model}}} = \kappa_{\text{CB}} - i\omega C_{\text{C}} + \frac{-i\omega\left(C_{\text{S}} + \frac{C_{1\text{N}}}{-i\omega T_{11}+1} + \frac{C_{2\text{N}}}{-i\omega T_{22}+1}\right)\kappa_{\text{CS}}}{-i\omega\left(C_{\text{S}} + \frac{C_{1\text{N}}}{-i\omega T_{11}+1} + \frac{C_{2\text{N}}}{-i\omega T_{22}+1}\right) + \kappa_{\text{CS}}}, \tag{S1}$$

where T_{11} and T_{22} are the spin-lattice relaxation times for In and Co, respectively. We have assumed that the cross-relaxation rate $1/T_{12}$ [7, 8] is zero.

Detailed investigation of the two-component nuclear specific heat as well as effects of cross-relaxation is beyond the scope of this work. We now show that in TISP measurements, inclusion of these effects does not affect the magnitude of the electronic specific heat and the nuclear spin-lattice relaxation rates at the level of accuracy necessary for the discussion in the main text.

The weak sensitivity of the magnitude of C_{S} and T_1 to changes in the nuclear system

is rooted in the fact that in TISP measurements, the nuclear specific heat $C_{\rm N}$ and the electronic specific heat $C_{\rm S}$ are determined independently by the frequency-dependent thermal impedance. For example, *if* the calorimeter-sample assembly is described by the single-isotope thermal impedance (Eq. (M2) in the Methods), then *any* changes in the magnitude of the nuclear specific heat $C_{\rm N}$ have *zero* effect on the magnitude of all other parameters, including that of $C_{\rm S}$ and T_1.

As a consequence of such "robustness", even when we modify the nuclear subsystem in a more significant way, such as the two-isotope (Eq. (S1)) versus single-isotope (Eq. (M2) in the Methods), the differences in the values of $C_{\rm S}$ and T_1 determined from fits to the two models are parametrically smaller than the differences in the parameters of the nuclear subsystem, as long as the latter are relatively small (see Supplementary Note 3 for mathematical details).

Specifically, for $CeCoIn_5$, the nuclear specific heat consists of 13% ^{59}Co and 87% $^{113/115}$In and the nuclear spin-lattice relaxation rate of ^{59}Co is about five times smaller than that of $^{115/113}$In (Fig. S8) [9, 10]. The relatively small, 13% "redistribution" of the nuclear specific heat components in Eq. (S1) has much smaller, less than 1%, effect on the magnitude of the electronic specific heat and 5% to 10% effect on the spin-lattice relaxation rate.

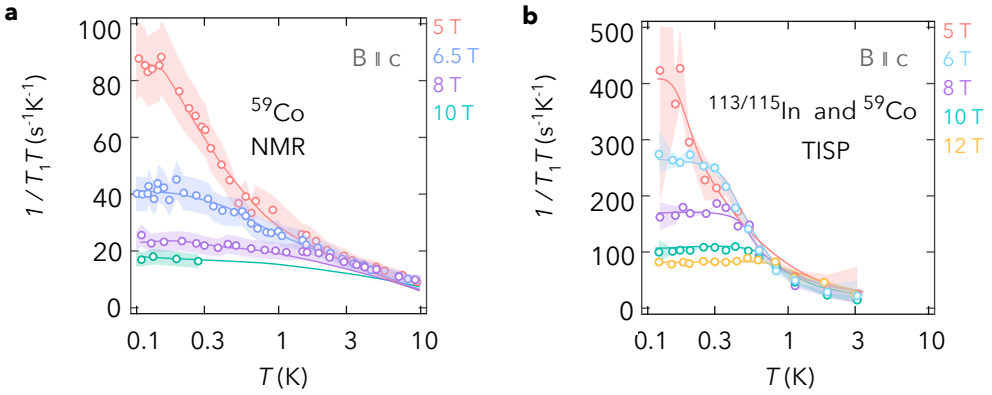

FIG. S8. **NMR measurements of $1/T_1T$ for ^{59}Co in $CeCoIn_5$ and TISP measurements of $1/T_1T$ for $CeCoIn_5$. a**. Nuclear spin-lattice relaxation rate of ^{59}Co in $CeCoIn_5$ from NMR measurements [9] for magnetic fields along the c-axis. **b**. TISP measurements of $1/T_1T$ for $CeCoIn_5$ from Fig. 2 of the main text.

To investigate the effects of two nuclear components, consider a system described by Eq. (S1) with a fixed set of 9 parameter. We take the corresponding thermal impedance

spectrum $\zeta(\omega)_2$ and use the single-isotope model (Eq. (M2) in the Methods) to fit six parameters, including $C_{\rm S}, C_{\rm N}$, and T_1. This defines the differences $\sigma_\eta(C_S)$, $\sigma_\eta(C_{\rm N})$, $\sigma_\eta(T_1)$ between the values obtained by such fit and the corresponding model parameters in Eq. (S1) of the more realistic model. To calculate the σ_η's we set

$$\begin{aligned} T_{11} &= T_1, \\ T_{22} &= 5T_1 \\ C_{2\rm N} &= 0.13 C_{\rm N} \\ C_{1\rm N} &= 0.87 C_{\rm N} \end{aligned} \tag{S2}$$

where the left side corresponds to the values in Eq. (S1) and the right-hand side corresponds to the values in the single-isotope model (Eq. (M2) in the Methods). The errors $\sigma_\eta(C_S)$, $\sigma_\eta(C_{\rm N})$, $\sigma_\eta(T_1)$, evaluated at four different temperatures, are given in table I.

T (K)	$\sigma_\eta(C_S)$ %	$\sigma_\eta(1/T_1T)$ %	$\sigma_\eta(C_{\rm N})$ %
0.12	0.2	7	5
0.35	0.03	6	7
1.1	0.001	5	7
3.0	0.001	4	8

TABLE I. **Errors introduced by 6-parameter model.** Errors introduced by the use of a single nuclear component, evaluated at a magnetic field of 12 T along the *ab*-plane.

As indicated above, the values of $\sigma_\eta(C_S)$ at temperatures above 0.3 K are much smaller than the nominal difference in the nuclear specific heat $\sigma_\eta(C_{\rm N})$. Importantly, the difference in C_S remains small at even lower temperatures due to the near perfect orthogonality in the parameter space (see Supplementary Note 3 for further details).

Supplementary Note 2:

Nuclear heat capacity

The nuclear specific heat is described by the high-temperature tail of a Schottky anomaly,

$$C_{\mathrm{N}} = (B/T)^2 c_0\,, \tag{S3}$$

where

$$c_0 = (1/3)\, N_{\mathrm{A}} k_{\mathrm{B}} \sum_n a_n I_n (I_n + 1)(g_n \mu_{\mathrm{N}}/k_{\mathrm{B}})^2 \tag{S4}$$

is the "reduced" nuclear specific heat, i.e., its value at 1 T and 1 K. The sum in Eq. (S4) is over all nuclear species with nuclear spin in the unit cell, a_n is the number of such atoms in each unit cell. I_n and g_n are their spin and nuclear g-factors, and $\mu_{\mathrm{N}} = 32.5$ neV/T is the nuclear magneton. A small quadrupolar contribution from In becomes important only at very low fields (below 100 mT). The value of the reduced nuclear specific heat, $c_0 = 85\ \mu$JK/molT^2, is determined in $CeCoIn_5$ by five ^{115}In and ^{113}In nuclei (which have the same nuclear spin and very close values of the nuclear g-factor [11]) and one ^{59}Co nuclei in each unit cell. ^{59}Co accounts for about 13% of the total nuclear specific heat both because of a smaller number of cobalt atoms and because of its smaller nuclear spin [11].

At low temperatures and high magnetic fields, the measured nuclear specific heat deviates from its expected value, through an additional factor $(1+K)^2$ related to the knight shift K,

$$C_{\mathrm{N}} = (1+K)^2\,(B/T)^2 c_0, \tag{S5}$$

describing enhanced – or screened – magnitude of local magnetic field $(1+K)B$. Figure S9 shows $(1+K)^2$ for all fields and temperatures in Fig. 2 in the main text. At low temperatures, the nuclear specific heat deviates away from its nominal value ($K = 0$) by as much as a factor of two, corresponding to values of K up to $\pm 30\%$ (see Fig. S10). We currently do not exclude that some of the observed effect can arise from measurement errors and the evaluation errors due to the 6-parameter fit with a single nuclear contribution. We note, however, that such errors associated with calibration should be independent of the magnetic field orientation.

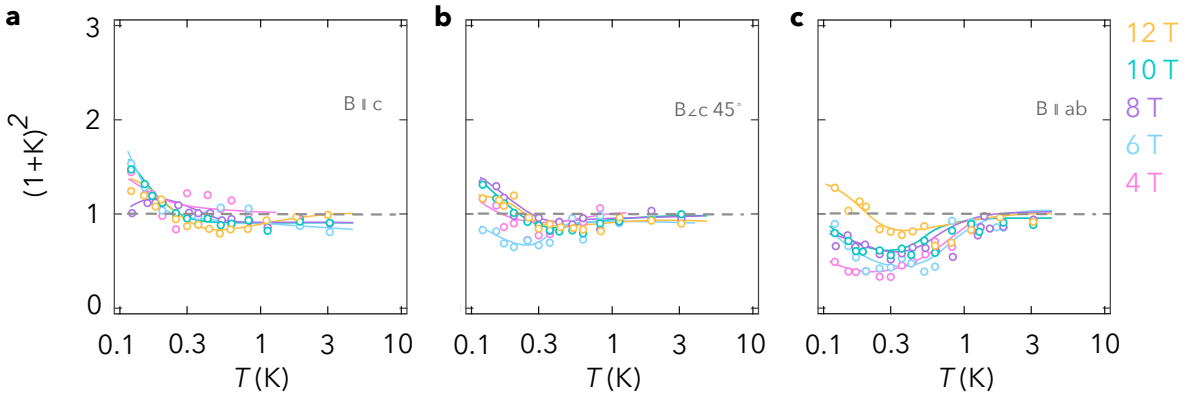

FIG. S9. **Measured nuclear specific heat normalized by its nominal value, Eq. (S3). a,b,c.** Nuclear specific heat (normalized by its nominal value, Eq. (S3)) for different magnetic fields and field orientations. The nuclear specific heat approaches its nominal value ($K = 0$, dashed line) at high temperatures. The deviations from the nominal value at lower temperatures indicate a difference between the applied magnetic field and the effective magnetic field at the nucleus.

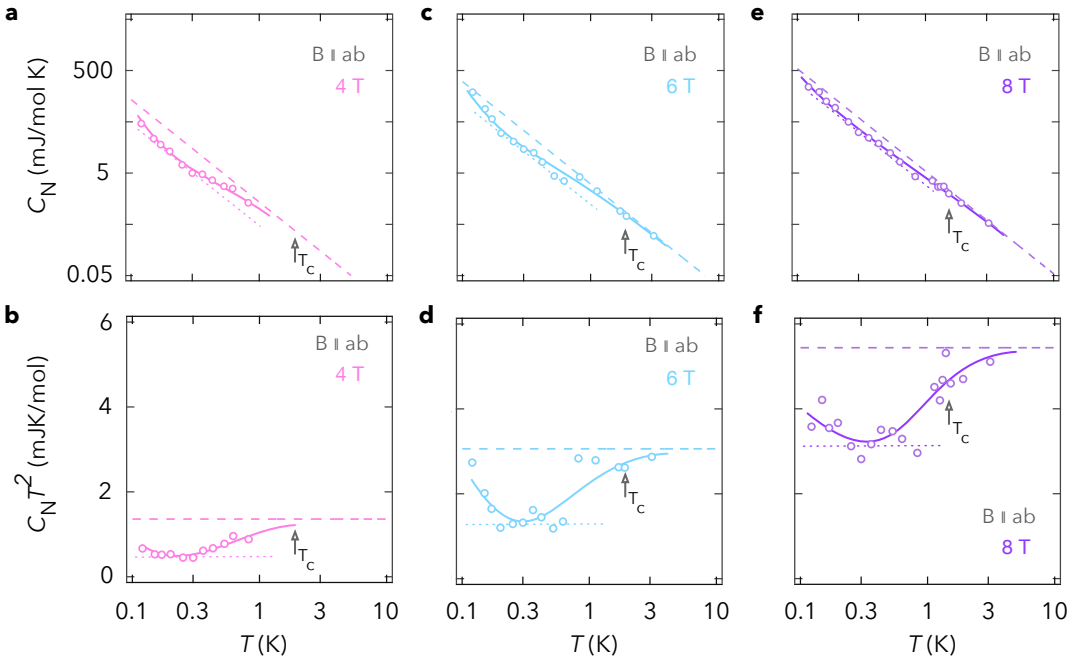

FIG. S10. **Temperature dependence of the nuclear specific heat in the superconducting and normal state of $CeCoIn_5$. a,c,e.** Temperature dependence of the nuclear specific heat for fields 4, 6, and 8 T along the *ab*-plane. The dashed line indicates the nominal ($K = 0$) value of nuclear specific heat. The dotted line indicates the maximum deviation of nuclear specific heat below the nominal value, more than a factor two smaller. Vertical arrows indicate the superconducting transition determined from Fig. S3. All solid lines are guides for the eye. **b,d,f.** Nuclear specific heat in a,c,e plotted as $T^2 C_{\mathrm{N}}$. The dashed line indicates the nominal behavior.

Supplementary Note 3:

Linear algebra of multiple nuclear species

The "orthogonality" of parameter space noted in Supplementary Note 1 is based on the following mathematical analysis. To cast the problem into a linear-space language we denote the observed thermal impedance spectra as $Z(\omega)$ and the model as $X(\omega)_{\lambda_i}$. Both are vectors in the linear space of functions of frequency. We define a scalar product

$$\langle A(\omega)|B(\omega)\rangle \tag{S6}$$

in this vector space via the frequency integrals

$$\int d\omega\beta(\omega)\, A(\omega)^* B(\omega)\,. \tag{S7}$$

where $\beta(\omega)$ is a given weight function. The goodness function (Methods) is represented by

$$g(\{\lambda_i\}) = \langle Z(\omega) - X(\omega)_{\lambda_i}|Z(\omega) - X(\omega)_{\lambda_i}\rangle\,. \tag{S8}$$

For a perfect fit of $Z(\omega)$ with $X(\omega)_{\lambda_i}$, the goodness function is at a minimum value equal to zero for small changes of all λ_i away from their best fit value λ_i^0. Now assume that the physical behavior $Z(\omega)$ is different from the one described by the model $X(\omega)_{\lambda_i}$. Let the observed behavior be $Z(\omega) + a\eta(\omega)$, where a is a small number and $\eta(\omega)$ is a function describing the deviation from the model $X(\omega)_{\lambda_i}$. We assume that $Z(\omega)$ is equal to the model $X(\omega)_{\lambda_i}$ for some parameters λ_i^0 but $Z(\omega) + a\eta(\omega)$ is not equal to $X(\omega)_{\lambda_i}$ for any set of λ_i. If we do the linear regression of $Z(\omega) + a\eta(\omega)$ using the model $X(\omega)_{\lambda_i}$, we would find best fit parameters $\lambda_i = \lambda_i^0 + d\lambda_i$ instead of λ_i^0. What is the relation between $d\lambda_i$, a, and $\eta(\omega)$?

Define the new best-fit parameters from

$$\begin{aligned} \Big\langle Z(\omega) + a\eta(\omega) - X(\omega)_{\lambda_i}\Big| Z(\omega) + a\eta(\omega) - X(\omega)_{\lambda_i}\Big\rangle &\to \min \\ \frac{d}{d\lambda_i}\Big\langle Z(\omega) + a\eta(\omega) - X(\omega)_{\lambda_i}\Big| Z(\omega) + a\eta(\omega) - X(\omega)_{\lambda_i}\Big\rangle &= 0 \end{aligned} \tag{S9}$$

We will only consider small values of a, for which we can truncate the expansion at the linear term,

$$\lambda_i = \lambda_i^0 + a\frac{d\lambda_i}{da}\,, \tag{S10}$$

i.e., we assume that $d\lambda_i$ are proportional to a. The problem is to find a set of derivatives $d\lambda_i/da$. Equation (S9) has a form,

$$\left\langle \frac{dX(\omega)_{\lambda_i}}{d\lambda_i} \middle| Z(\omega) + a\eta(\omega) - X(\omega)_{\lambda_i} \right\rangle = 0\,. \tag{S11}$$

If a is zero, the ket in Eq. (S11) is identically zero for $\lambda_i = \lambda_i^0$. The set of six functions

$$V_i(\omega) = \left(\frac{dX(\omega)_{\lambda_i}}{d\lambda_i} \right)_{\lambda_i = \lambda_i^0} \tag{S12}$$

near λ_i^0 defines a six-dimensional "tangent" linear space at $Z(\omega) = X(\omega)_{\lambda_i^0}$. Equation (S11) can only constraint parameters a and $d\lambda_i/da$ as long as the function $\eta(\omega)$ can be decomposed into this tangent space. This is because small changes in λ_i away from λ_i^0 produce changes in the functions $X(\omega)_{\lambda_i}$ that lie in tangent space, $\delta X(\omega) = d\lambda_i V_i(\omega)$. Therefore we need to distinguish two orthogonal components of function $\eta(\omega)$,

$$a\eta(\omega) = a\eta(\omega)_\perp + a\eta(\omega)_\parallel\,, \tag{S13}$$

where $a\eta(\omega)_\parallel$ is in the tangent space

$$\eta(\omega)_\parallel = \sum_i V_i(\omega)\ \eta_i \tag{S14}$$

with the expansion coefficients η_i whereas $\eta(\omega)_\perp$ is orthogonal to the tangent space,

$$\left\langle \eta(\omega)_\perp \middle| V_i(\omega) \right\rangle = 0 \qquad \text{for all } i. \tag{S15}$$

With this, Eq. (S11), is only sensitive to the tangent component $\eta(\omega)_\parallel$.

The coefficients η_i in Eq. (S14) are given by

$$\eta_i = K_{ij} \left\langle \eta(\omega) \middle| V_j(\omega) \right\rangle\,, \qquad K_{ij} = \left(\left\langle V_i(\omega) \middle| V_j(\omega) \right\rangle \right)^{-1} \tag{S16}$$

where matrix K_{ij} accounts for non-orthogonality of the basis $V_i(\omega)$ in the tangent space.

Equation (S11) now states that the tangent space component of $\eta(\omega)_\parallel$ must be "balanced" by the small changes in the fitting parameters, which immediately results in

$$\frac{d\lambda_i}{da} = \eta_i\,. \tag{S17}$$

where η_i is given by Eq. (S16).

A check of this result is that when the function $\eta(\omega)$ coincides with one of the basis vectors $V_i(\omega)$ (i.e., the modified $Z(\omega)+a\eta(\omega)$ is still described exactly by the model $X(\omega)_{\lambda_i}$ with simple shift in the fitting parameters), only one of $d\lambda_i$ must be nonzero, i.e.,

$$\frac{d\lambda_i}{d\lambda_j} = \delta_{ij} \tag{S18}$$

This is indeed satisfied because

$$\sum_j K_{ij} \left\langle V_i(\omega) \middle| V_j(\omega) \right\rangle = \delta_{ij} \tag{S19}$$

---

[1] R. Movshovich, M. Jaime, J. D. Thompson, C. Petrovic, Z. Fisk, P. G. Pagliuso, and J. L. Sarrao, "Unconventional Superconductivity in $CeIrIn_5$ and $CeCoIn_5$: Specific Heat and Thermal Conductivity Studies," Phys. Rev. Lett. **86**, 5152 (2001).

[2] S. Ikeda, H. Shishido, M. Nakashima, R. Settai, D. Aoki, Y. Haga, H. Harima, Y. Aoki, T. Namiki, H. Sato, and Y. Onuki, "Unconventional superconductivity in $CeCoIn_5$ studied by the specific heat and magnetization measurements," J. Phys. Soc. Japan **70**, 2248 (2001).

[3] G. Sparn, R. Borth, E. Lengyel, P. G. Pagliuso, J. L. Sarrao, F. Steglich, and J. D. Thompson, "Unconventional superconductivity in $CeCoIn_5$, a high pressure study," Physica B: Condensed Matter **319**, 262 (2002).

[4] K. An, T. Sakakibara, R. Settai, Y. Onuki, M. Hiragi, M. Ichioka, and K. Machida, "Sign reversal of field-angle resolved heat capacity oscillations in a heavy fermion superconductor $CeCoIn_5$ and $d_{x^2-y^2}$ pairing symmetry," Phys. Rev. Lett. **104**, 037002 (2010).

[5] J. S. Kim, D. Bedorf, and G. R. Stewart, "Effect of Disorder Induced by Heavy-Ion Irradiation on $CeCoIn_5$ Superconductivity," Journal of Low Temperature Physics **157**, 29 (2009).

[6] E. Lengyel, R. Borth, P. G. Pagliuso, J. Sarrao, G. Sparn, F. Steglich, and J. D. Thompson, "Heat Capacity Under Pressure of $CeCoIn_5$," High Pressure Research **22**, 185 (2002).

[7] A. Abragam, *The principles of nuclear magnetism* (Oxford university press, 1961).

[8] L. C. Hebel, "Spin Temperature and Nuclear Relaxation in Solids," Solid State Physics **15**, 409 (1963).

[9] H. Sakai, S. E. Brown, S-H. Baek, F. Ronning, E. D. Bauer, and J. D. Thompson, "Magnetic-Field-Induced Enhancements of Nuclear Spin-Lattice Relaxation Rates in the Heavy-Fermion

Superconductor $CeCoIn_5$ Using ^{59}Co Nuclear Magnetic Resonance," Phys. Rev. Lett. **107**, 137001 (2011).

[10] M. Yashima, S. Kawasaki, Y. Kawasaki, G.-Q. Zheng, Y. Kitaoka, H. Shishido, R. Settai, Y. Haga, and Y. Onuki, "Magnetic criticality and unconventional superconductivity in $CeCoIn_5$: Study of ^{115}In-nuclear quadrupole resonance under pressure," J. Phys. Soc. Japan **73**, 2073 (2004).

[11] N. J. Stone, "Table of nuclear magnetic dipole and electric quadrupole moments," INDC, International Nuclear Data Committee INDC **(NDS)-0658 Distr** (2014).